PNAS RESEARCH ARTICLE | EARTH, ATMOSPHERIC, AND PLANETARY SCIENCES OPEN ACCESS

Accretion of the cratonic mantle lithosphere via massive regional relamination

Zhensheng Wang[a,1], Fabio A. Capitanio[a,b], Zaicong Wang[a], and Timothy M. Kusky[a,c,1]

Edited by T. Harrison, University of California Los Angeles, Los Angeles, California; received January 24, 2022; accepted August 13, 2022

Continental, orogenic, and oceanic lithospheric mantle embeds sizeable parcels of exotic cratonic lithospheric mantle (CLM) derived from distant, unrelated sources. This hints that CLM recycling into the mantle and its eventual upwelling and relamination at the base of younger plates contribute to the complex structure of the growing lithosphere. Here, we use numerical modeling to investigate the fate and survival of recycled CLM in the ambient mantle and test the viability of CLM relamination under Hadean to present-day mantle temperature conditions and its role in early lithosphere evolution. We show that the foundered CLM is partially mixed and homogenized in the ambient mantle; then, as thermal negative buoyancy vanishes, its long-lasting compositional buoyancy drives upwelling, relaminating unrelated growing lithospheric plates and contributing to differentiation under cratonic, orogenic, and oceanic regions. Parts of the CLM remain in the mantle as diffused depleted heterogeneities at multiple scales, which can survive for billions of years. Relamination is maximized for high depletion degrees and mantle temperatures compatible with the early Earth, leading to the upwelling and underplating of large volumes of foundered CLM, a process we name massive regional relamination (MRR). MRR explains the complex source, age, and depletion heterogeneities found in ancient cratonic lithospheric mantle, suggesting this may have been a key component of the construction of continents in the early Earth.

craton | lithospheric mantle | mantle heterogeneities | relamination

Significance

The continental lithospheric mantle contains regionally distinct domains with different ages, compositions, and sources, recording diverse formation mechanisms. Geodynamics modeling demonstrates that the delamination of depleted older and unrelated exotic continental lithospheric mantle allows sinking and mixing with the mantle. The multiscale heterogeneities formed retain most of the original chemical buoyancy and are embedded beneath distant plates in massive regional relamination (MRR) events. MRR events occurred episodically for tens to hundreds of Myr and likely contributed to the formation of most of the continental lithospheric mantle . The models provide constraints on the distribution, size, transportation, timescale, mixing, and relamination of different continental lithospheric mantle relicts throughout Earth's history.

Continents keep the record of the evolution of our planet and the life it hosts. How continents formed and evolved remains, to date, an outstanding question in geosciences (1–3). Several lines of evidence show that continents are gradually accreted from their interiors to their margins, from Precambrian cratonic cores to marginal orogens (4). However, how the cratonic cores are formed is controversial, and proposed models invoke processes related to plate margins, such as rifting, subduction and stacking, accretion, and evolution along arc-like environments, or to mantle plumes (1, 2, 5–7), all providing compatible petrogenetic environments. Cratons have increased buoyancy and rigidity that allowed stabilization and preservation (1–3); however, the heterogeneous composition supports the idea that recycling, magmatic addition, reworking, and refertilization are common during their formation (8–10). Evidence from the geological record of cratons shows that ancient lithospheric roots comprise large volumes of harzburgite and depleted lherzolite with highly heterogeneous ages, compositions, and sources (3, 5, 9, 11, 12). Similar heterogeneities are found in younger orogenic and oceanic regions, where evidence from geological and geophysical studies shows ancient, depleted peridotites embedded within or beneath younger fertile peridotites (13–16). This provides proof that the embedding of delaminated, exotic, older, and depleted mantle in the growing lithosphere is a relevant component of the evolution of the Earth's outer shell (13, 14, 17, 18), potentially contributing to the construction of the continents.

Delamination of the older continental lithospheric mantle is a fundamental process of continental evolution, compatible with different tectonic regimes, resulting in lithospheric thinning and craton destruction and critically defining the nature and evolution of mantle heterogeneities (2, 5, 12, 17, 19–22). The cycle of mantle heterogeneities is best understood as a large-scale process involving sinking and mixing of variable volumes of CLM, as well as the upwelling of CLM residue (18), driven by long-lasting chemical buoyancy, and its eventual embedding in the growing lithosphere. The subsequent upwelling of CLM residue and relamination of the new lithosphere may contribute to the characteristic source, age, and compositional heterogeneities of cratons. To date, the viability, conditions, effects, and significance of subsequent relamination through time remain poorly addressed.

The conditions controlling sinking, upwelling, and relamination of foundered CLM (in other words, its fate and survival) are strictly related to the initial lithospheric

Author contributions: Zhensheng Wang and T.M.K. designed research; Zhensheng Wang performed research; Zhensheng Wang and F.A.C. contributed new analytic tools; Zhensheng Wang, F.A.C., Zaicong Wang, and T.M.K. analyzed data; and Zhensheng Wang, F.A.C., Zaicong Wang, and T.M.K. wrote the paper.

The authors declare no competing interest.

This article is a PNAS Direct Submission.

[1]To whom correspondence may be addressed. Email: jasonwang@cug.edu.cn or tkusky@gmail.com.

This article contains supporting information online at http://www.pnas.org/lookup/suppl/doi:10.1073/pnas.2201226119/-/DCSupplemental.

Published September 19, 2022.

buoyancy and the mantle viscosity, mainly functions of CLM size, composition, and temperature (23, 24). The majority of depleted, cold CLM is compositionally buoyant (25) but achieves negative buoyancy due to thermal contraction; thus, once decoupled, it founders into the ambient mantle. Once in the ambient mantle, compositional buoyancy may counteract the vanishing thermal negative buoyancy, opposing sinking, allowing the foundered CLM to rise and relaminate the base of the growing lithosphere (13, 17, 18). The complex feedback between mantle flow, heat transfer, viscosities, and thermal and compositional buoyancy provides key constraints on the spatio-temporal evolution of foundered CLM, including its sinking, transportation, stagnation, upwelling, relamination, and deep mixing, relevant to the interpretation of the physical and chemical mantle anomalies at different depths (17, 20, 26–30).

The conditions for sinking and upwelling, controlling relamination, are critically impacted by mantle temperatures and may have changed under hotter mantle conditions in the early Earth. Throughout Earth's evolution, the mantle potential temperature (T_p) has changed; in turn, this may have affected the size of the delaminated lithosphere through its thermal as well as chemical buoyancy, function of the depletion degree (F), rheological properties of the mantle, and plate surface velocity (V_{surf}) as a result of thermal convection vigor (6, 7, 25, 31). Therefore, the force balance of foundered CLM has changed accordingly, resulting in different possible scenarios for the fate of foundered CLM, ranging from complete mixing in the ambient mantle to survival and embedding in the new lithosphere (17, 23, 26, 29, 32). Here, we used thermo-chemo-mechanical modeling (*SI Appendix*, sections 1 and 2) to reproduce different conditions throughout Earth's past and address cycles of CLM recycling with a focus on its relamination. We investigated the conditions for CLM relamination viability, assessing the paths and fates of foundered CLM segments in the mantle, which include upwelling, stagnation depth and timescale, and partitioning between relamination and mixing. We then focused on the complexities this process adds to the growing lithospheric lid, highlighted by the lithosphere's heterogeneous structure, and compared the model results with realistic lithosphere structures to discuss the significance of CLM relamination in the construction of the existing lithosphere.

Results

Earth's history shows a variation of mantle T_p from the Hadean to the present (31, 33). We therefore designed models with a ΔT_p covering the range of mantle T_p difference with respect to the present day from 0 to greater than +300 °C (31). We considered a CLM block, detached from its crust (18, 34), and simulated the sinking processes that do not rely on early Earth tectonic regimes (35–38) or different foundering triggers (39, 40). We did not address the initial conditions leading to the formation of the CLM (5–7, 41) but instead tested a range of different CLM masses related to depletion and CLM shape. The average depletion degrees of the CLM vary as $F = 0$ to 50%, covering the values observed, ranging from the primitive to the highly depleted mantle (8, 42). These parameters are embedded in the model through a temperature- and depletion-dependent equation of state (density) (25) (*SI Appendix*, section 1). The second parameter tested was the delaminated CLM block shape, length (50 to 500 km), and thickness (40 to 160 km), which may determine the Stokes sinking velocity and the survival of the thermal anomaly in the mantle (18, 43). The models additionally tested other parameters, including plate surface velocity (V_{surf} = 0 to 10 cm/y) and maximum mantle viscosity ($\eta_{max} = 10^{23}$ to 10^{26} Pas) to represent plate velocity variations (35, 36) and different lithospheric strengths (44, 45), respectively. The mantle weakening factor (f_{vis} = 0.1 to 1.0) was also tested, which reproduced the effect of melt and fluids (44). This approach followed similar setups in previous works investigating the sinking of foundered lithosphere in the mantle (18, 43), where similarly simplified initial shapes were adopted. We designed a reference group with a model setup including a thick (160 km) cratonic block sinking in the dry ambient mantle, with no water- or fluid-related weakening, following previous works (18, 44). A second group aimed to test the sensitivity of the model to the parameters above (*SI Appendix*, section 3).

The Relamination of CLM. All models showed similar evolution, including the following stages (Fig. 1). In the first stage, the detached CLM sinks and stagnates in the mantle (Fig. 1 *A*–*C*, *G*–*I*, and *M*–*O*) until the thermal negative buoyancy has vanished, and then evolution is driven by the residual compositional buoyancy. In the second stage, the CLM is partly mixed and sheared in the mantle, and then portions of residue with different sizes (kilometer to 100-km level) ascend in pulses. This stage is characterized by upwelling in short ∼10-Myr episodes, lasting for a total of ∼100 to 200 Myr. At the end of this stage, variable volumes of CLM have kept their maximum concentration and upwelled to relaminate the bottom of the drifting lithosphere, while the remainder has mixed with the ambient mantle (Fig. 1 *D*, *E*, *J*, *K*, *P*, and *Q*). In the final stage, the configuration is stable (Fig. 1 *F*, *L*, and *R*), in which the relaminated CLM remains embedded in the lithosphere until the end of the modeled time, 1,200 Myr. This process is similar to the relamination of delaminated or subducted crust (46, 47), but it does not require subduction and involves deep-sourced mantle material and affects wider and deeper regions than the relamination in subduction mantle wedges. We thus defined the large-scale relamination of the CLM under the growing lithosphere as massive regional relamination (MRR).

Although foundered CLM segments have similar recycling processes, the timing of their evolution, the MRR onset time, the stagnation depth, and the partition ratio between relamination and mixing differ and are controlled by the parameters tested here. These differences reflect the changing distribution and concentration of CLM materials in different models (Fig. 2). We showed that the viability of relamination is mainly dependent on F and ΔT_p (Figs. 2 and 3*A*). For $F \geq 40\%$ and $\Delta T_p \leq 50$ °C, the chemical buoyancy overcame the thermal negative buoyancy and no sinking occurred (Fig. 2*A*). On the contrary, models with F = 0% had no chemical residual buoyancy once the thermal anomaly was diffused (Fig. 2*B*). In this case, upwellings were supported by convection; yet CLM relamination was negligible. Most models across the rest broad ΔT_p (50-300 °C) and the values of $F = 10$ to 40% tested supported the viability of the MRR (Figs. 2 *C*–*E* and 3*A*).

For thick (160-km) cratonic blocks sinking in the dry mantle (18), the evolution of the MRR is mainly controlled by F and ΔT_p, which determine CLM chemical and thermal buoyancy and the viscosity of the mantle. The range of inferred mantle temperatures and depletion degree of the CLM resulted in a broad spectrum of possible recycling and relamination behaviors (*SI Appendix*, section 4). The outcomes showing different paths, MRR onset times, stagnation depth, and partition ratios between relamination and mixing are addressed in the F-ΔT_p space (Fig. 3). We showed that the depletion degree F plays a critical role in the stagnation depth and MRR onset time

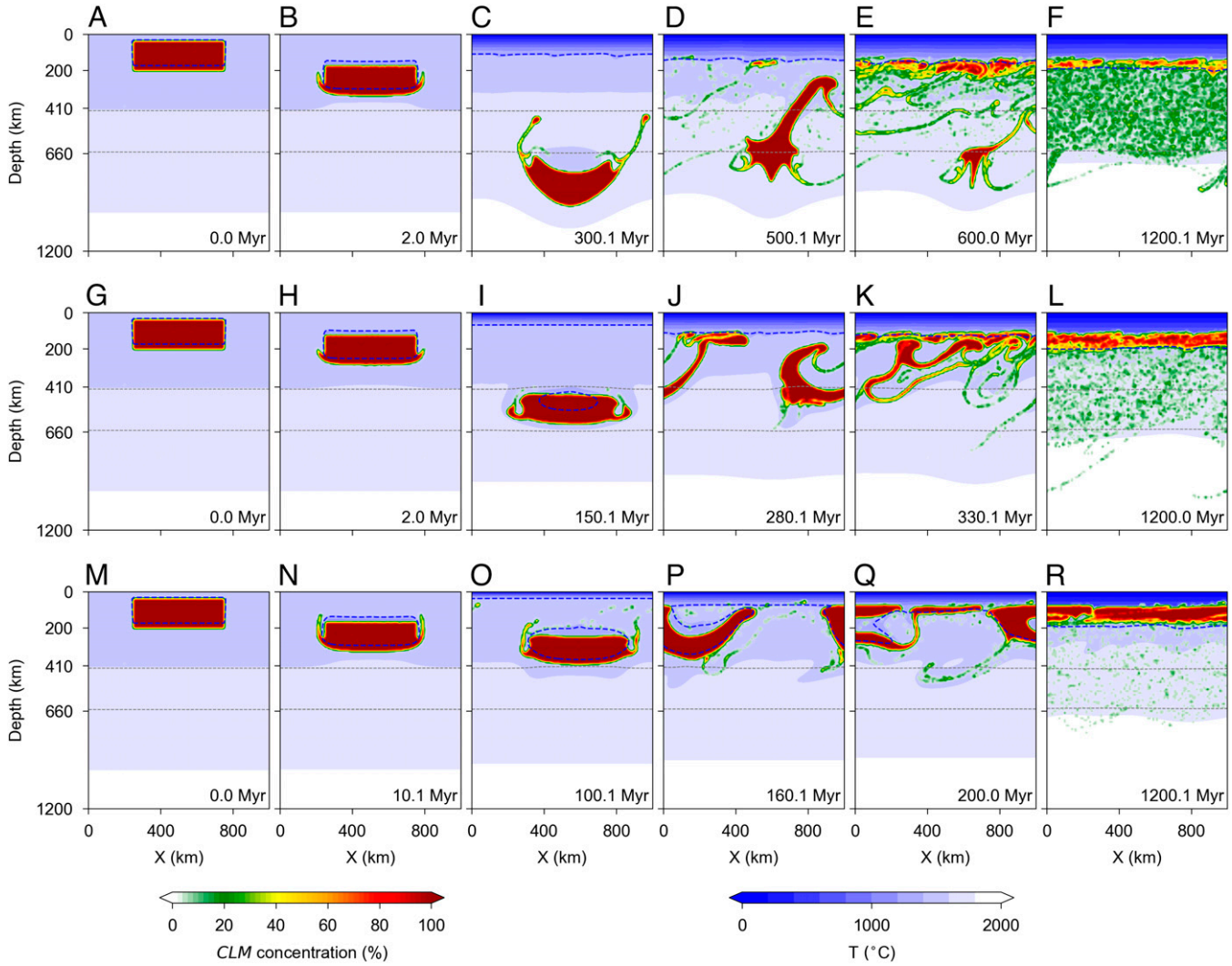

Fig. 1. Relamination of the CLM. (*A–R*) Different time steps of the numerical models with initial CLM depletion degree F = 10% (*A–F*), F = 20% (*G–L*), and F = 40% (*M–R*). ΔT_p is 150 °C, surface velocity is 3 cm/y, f_{vis} is 1.0, and maximum viscosity is 10^{25} Pas in all models. Dark dashed lines for the phase changes at 410- and 660-km depth; blue dashed lines for the 1,350 °C isotherm. Color scale with green to brown for the concentration of original CLM and in shades of blue for the temperature (T).

(Fig. 3 *A* and *B*), whereas the models are weakly dependent on ΔT_p. The depth of stagnation varied from 200 km to lower mantle depth with decreasing initial F and increasing T_p (Fig. 3*A*). Because small depletion degrees can lead to small CLM buoyancy and increasing ΔT_p reduces the mantle's viscous resistance against sinking, both can favor deeper sinking depths. The stagnation can last for tens to hundreds of Myr, and then evolution is dominated by episodic MRR events (Figs. 2 *C–E* and 3*A*). The initial MRR time varied from 100 to >1,200 Myr with decreasing initial F and T_p (Fig. 3*B*), also because small F and ΔT_p can reduce CLM buoyancy and relatively increase viscous resistance against upwelling, respectively. The initial MRR time of CLM with F = 30 to 50% was ∼100 to 400 Myr after delamination, whereas the initial MRR time of CLM with F = 0 to 20% ranged from 300 to >1,200 Myr (Fig. 3*B*). In such a long period, the lithosphere at the surface may move relative to the sinking CLM, thousands of kilometers, also at small surface velocity. Therefore, the MRR can embed relaminated CLM to the base of distant lithospheric plates. CLM partitioning between MRR and mantle was measured via the volume percentage of relaminated CLM relative to the total volume of CLM foundered. For CLM with F > 20%, the relaminated CLM accounted for 40 to 100% of the volume of the foundered CLM, increasing with increasing F and decreasing T_p values (Fig. 3*C*). For CLM with $F \leq$ 20%, the volume percentage of relaminated CLM was relatively small and mainly increased with increasing F (Fig. 3*C*).

Sensitivity tests (*SI Appendix*, section 3) showed the second-order control of initial CLM shape and f_{vis}, whereas the V_{surf} and maximum mantle viscosity (η_{max}) had negligible influence. The characteristic delaminated CLM block size is mostly determined by its thickness rather than its length, which is close to mantle lithosphere thickness (48). The size of the foundered CLM controls mostly the duration of the initial stages. The diffusion of initial small CLM blocks occurs more rapidly; then the thermal negative buoyancy is lost, and upwelling occurs earlier. The time until complete vanishing of thermal buoyancy takes ∼100 to 500 Myr depending on the size and temperature of the cold CLM and its initial depletion degree. Earlier vanishing of negative buoyancy of smaller initial blocks resulted in shallower sinking depth and smaller lithospheric fragments but also fed fewer upwelling episodes (*SI Appendix*, section 3). The f_{vis} may affect mantle viscosity and similarly impact the timing, although it may work in regions rich in melts or fluids (44).

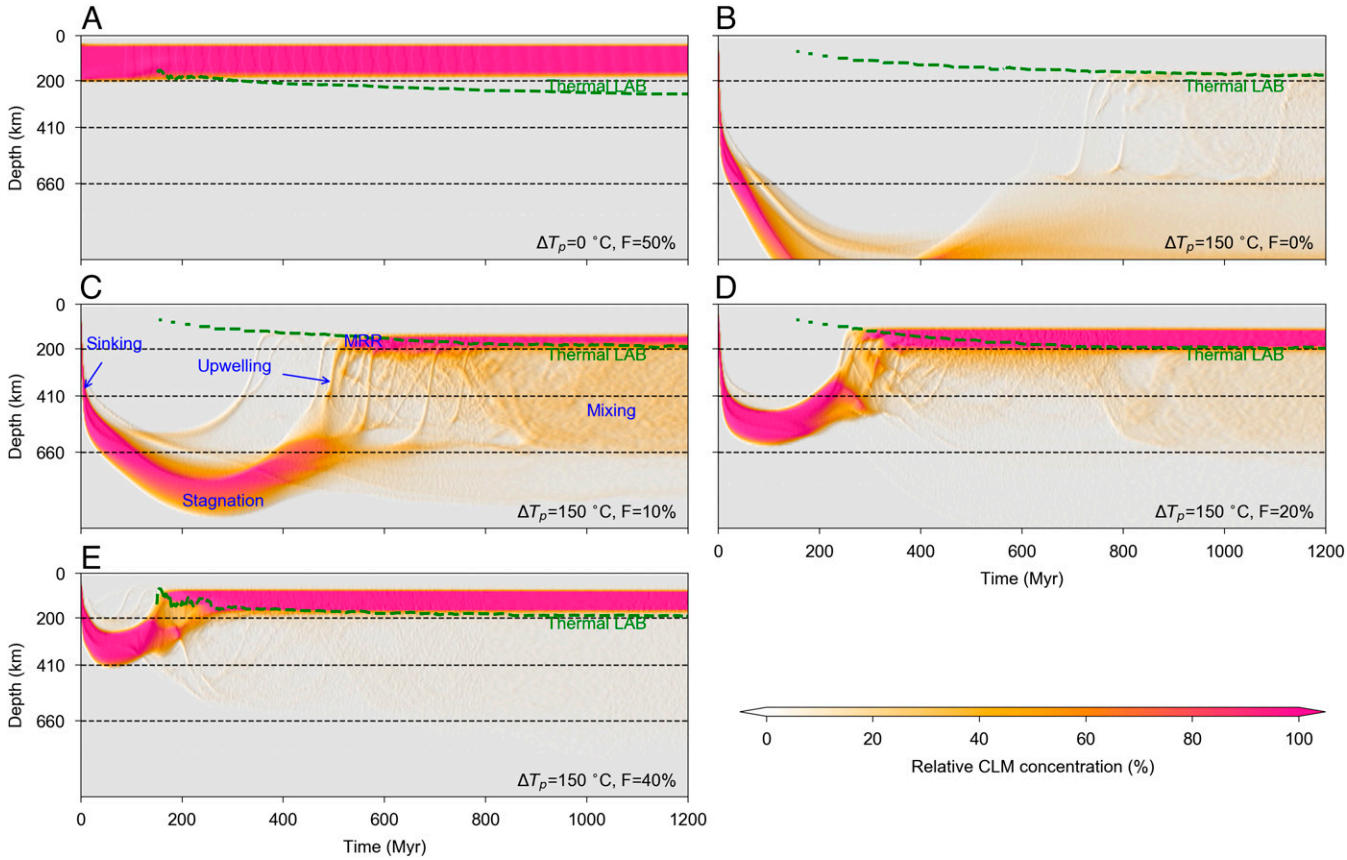

Fig. 2. Evolution of CLM recycling in the mantle. (*A*) No sinking. (*B*) CLM sinking into deep mantle without significant relamination. (*C*–*E*) CLM stagnates at different depths, *C* (*A*–*F* in Fig. 1), *D* (*G*–*L* in Fig. 1), *E* (*M*–*R* in Fig. 1). In white to red, the concentration of CLM tracers at a depth relative to their initial concentration at 40- to 160-km depth across the model in time. Green dashed lines represent the average depth of the 1,350 °C isotherm (thermal lithosphere-asthenosphere boundary [LAB]).

A weaker mantle rheology ($f_{vis} < 1.0$) can also lead to smaller lithospheric fragments, more frequent upwelling episodes, and stronger mixing (*SI Appendix*, section 3). Although the chosen parameters may influence sinking depth, CLM segment size, episode number, and duration of upwelling, they do not change the feasibility of relamination.

Lithospheric Composition, Structures, and Heterogeneities. The relamination and incorporation of CLM relicts into the growing lithospheric mantle lead to different compositions, with heterogeneous source, age distributions, and structures. The evolution and complexity of the final lithosphere architectures are due to the MRR and therefore are best understood in terms of ΔT_p and F controls. In models with $F = 0\%$, the compositional buoyancy of the delaminated CLM was negligible; thus, no relamination occurred. The growing lithosphere was not influenced by the MRR and had only a thin lithospheric layer extending to less than ∼130-km depth, with depletion degree and age decreasing uniformly with depth (Fig. 4 *A* and *B*). In models with large ΔT_p and F values, the previously delaminated CLM and the newly formed lithospheric lid were all depleted; thus, the depleted lid was relaminated by ancient CLM with different ages but no significant depletion degree variations. Thus, the embedded CLM formed a thick depleted root, trapping older materials in the lower part of the growing lithosphere (Fig. 4 *C* and *D*). In the models with large ΔT_p but small F values, the incorporated lithosphere exhibited a two-layer structure in both depletion and age, with an upper layer composed of newly formed young, depleted materials, and the lower layer was embedded by older fertile CLM materials (Fig. 4 *E* and *F*). In the models with small ΔT_p but large F values, the lithosphere also exhibited a two-layer structure in both depletion and age; in the top layer, young fertile material was found, whereas older depleted material concentrated in the bottom layer (Fig. 4 *G* and *H*). In the models with small ΔT_p and F values, the lithosphere had a thicker fertile root, with previously foundered fertile CLM relicts being relaminated below fertile growing lithosphere (Fig. 4 *I* and *J*).

Discussion

Our results, including the timescale and behaviors of relamination as well as the distribution and size of relaminated depleted mantle lithospheric relicts, are comparable to those of previous works (6, 7, 15, 18, 41). While recent works have mainly investigated the relamination of recycled CLM relicts to the Phanerozoic oceanic lithosphere (15, 18), we focused on its contribution to the accretion and reconstruction of continents through time. A test of the viability of relamination for the accretion of continental lithosphere is best provided by comparisons to the geological record of lithospheric heterogeneities proposed in this section. A survey of the age and composition structures of the lithosphere provides key evidence for the viability of processes of recycling and relamination through time.

Massive Regional Relamination: Constraints from Age Distribution. Lithospheric xenoliths derived from different tectonic units record a wide range of Re isotopic depletion ages, including many significantly older than those of the overlying crust, suggesting the inclusion of CLM relicts in the construction of the later lithosphere (9).

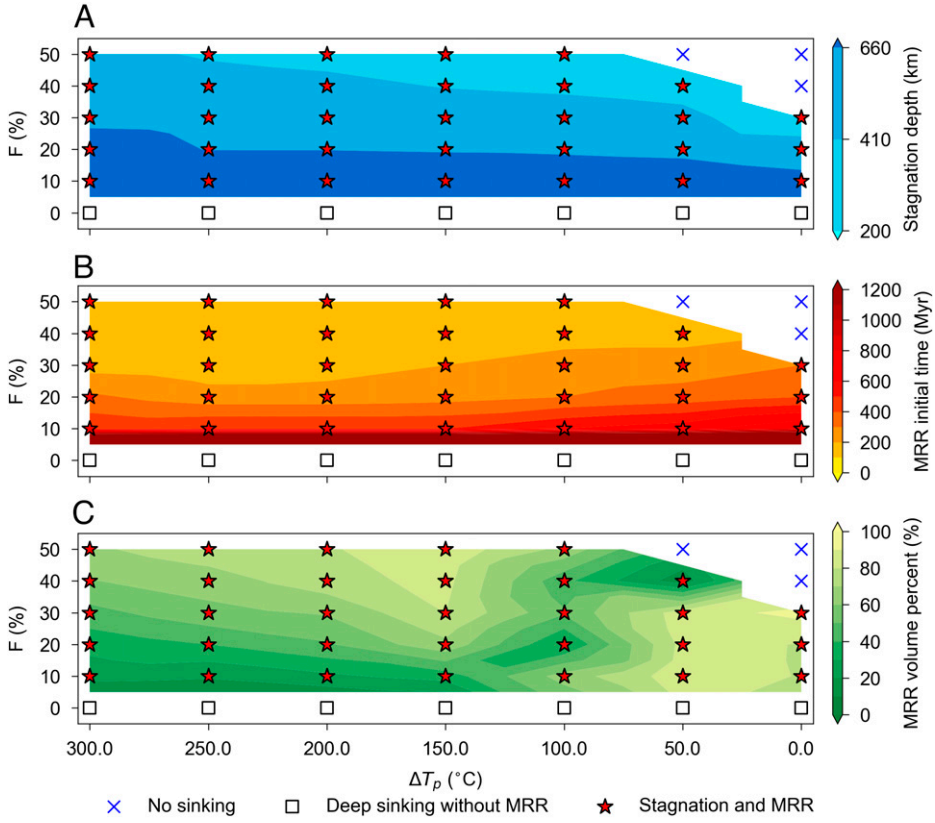

Fig. 3. CLM recycling evolution as a function of depletion degree F and excess temperature ΔT_p. (*A*) Stagnation depth. (*B*) MRR initial time. (*C*) Volume percentage of relaminated CLM reflecting the partition between relamination and mixing.

There is extensive evidence of Precambrian CLM relicts embedding in the construction of Phanerozoic oceanic and orogenic lithosphere. Proterozoic CLM relicts are found in Phanerozoic ophiolites in the Tethysides (49, 50), Precambrian CLM relicts are recorded in magmatic rocks in the Hawaiian islands (51), and different scales of ancient CLM fragments are recognized under the ridges and highlands in the Atlantic and Indian oceans (13, 15, 32, 52, 53) and beneath the Ontong Java oceanic plateau (14). The appearance of such ancient CLM materials in these areas implies that CLM must have delaminated from the ancient lithosphere, sank and mixed into the mantle, and been transported a great distance to be eventually embedded in the growing oceanic lithosphere and the orogenic lithosphere after ocean closure. Archean CLM relicts are also found under many Proterozoic crustal units, such as the 3.0- to 2.1-Ga CLM segments beneath the Proterozoic Halls Creek belts in Australia (11), and Archean melt extraction events are recorded beneath the Proterozoic regions of east Greenland (54). Collectively, this evidence supports the relamination process shown here.

According to the face values of Re-Os model ages from the existing lithosphere, some Archean cratonic lithosphere (Fig. 5 *A* and *B*) also exhibits special age patterns showing that ancient materials are located below or embedded within younger ones. For example, in the central part of the Slave Craton, 3.5- to 3.0-Ga CLM harzburgites are located beneath 3.0- to 2.7-Ga lherzolites, which are further overlain by a 2.6- to 2.75-Ga crust (Fig. 5*B*) (55, 56). Accordingly, such age heterogeneities, with sizes ranging from microscale to hundred-kilometer scale (Fig. 5*B*), seem to exist widely in the lithosphere from the early Archean to the Phanerozoic (9). These abnormal lithospheric age structures (e.g., Fig. 5 *A* and *B*) indicate that the lithospheric materials in these areas are actually derived from different regions with different ages, which cannot be explained by other lithospheric formation models in Fig. 6 *A*–*D*; however, they are consistent with the MRR proposed here for their sizes and complex age structures (Fig. 4 *B*, *D*, and *F*).

MRR can also explain other crust-mantle age decoupling, in which the lithospheric mantle and crustal ages cannot be easily reconciled. For example, Proterozoic lithospheric mantle segments are found below the Archean North China and Cask cratons (57, 58), and late Archean lithospheric mantle is found beneath Paleoarchean to Mesoarchean crustal units in the North Atlantic Craton (12). Such a composite lithosphere with an ancient upper part and a young lower part can be formed by MRR events only if the delaminated and upwelled CLM is much younger than the lithospheric lid, which is similar to the results of documented replacement (58) and stacking (59) according to their age structures. Although the age range of Archean CLM is mostly consistent with that of its overlying Archean crust (5), there are extensive mismatches in peak age values and distribution (3, 59), which suggest that the crust and mantle are not completely coupled. Considering the global similarity of Archean regions in their lithospheric and crustal age ranges (60), it cannot be ruled out that relamination and embedding of CLM might occur at the early stages of Archean craton formation.

The delamination and MRR model can also explain the lack of Hadean lithospheric mantle, as recorded by xenolith data (9, 61). From the Hadean to the early Archean, average ambient mantle temperatures were higher ($\Delta T_p >> 200\,^{\circ}C$), and recycled CLM relicts could have surpassed the solidus (Fig. 7*A*) (62). While this may lead to partial melting and further melt extraction, this could also over-print (or reset) the radiogenic

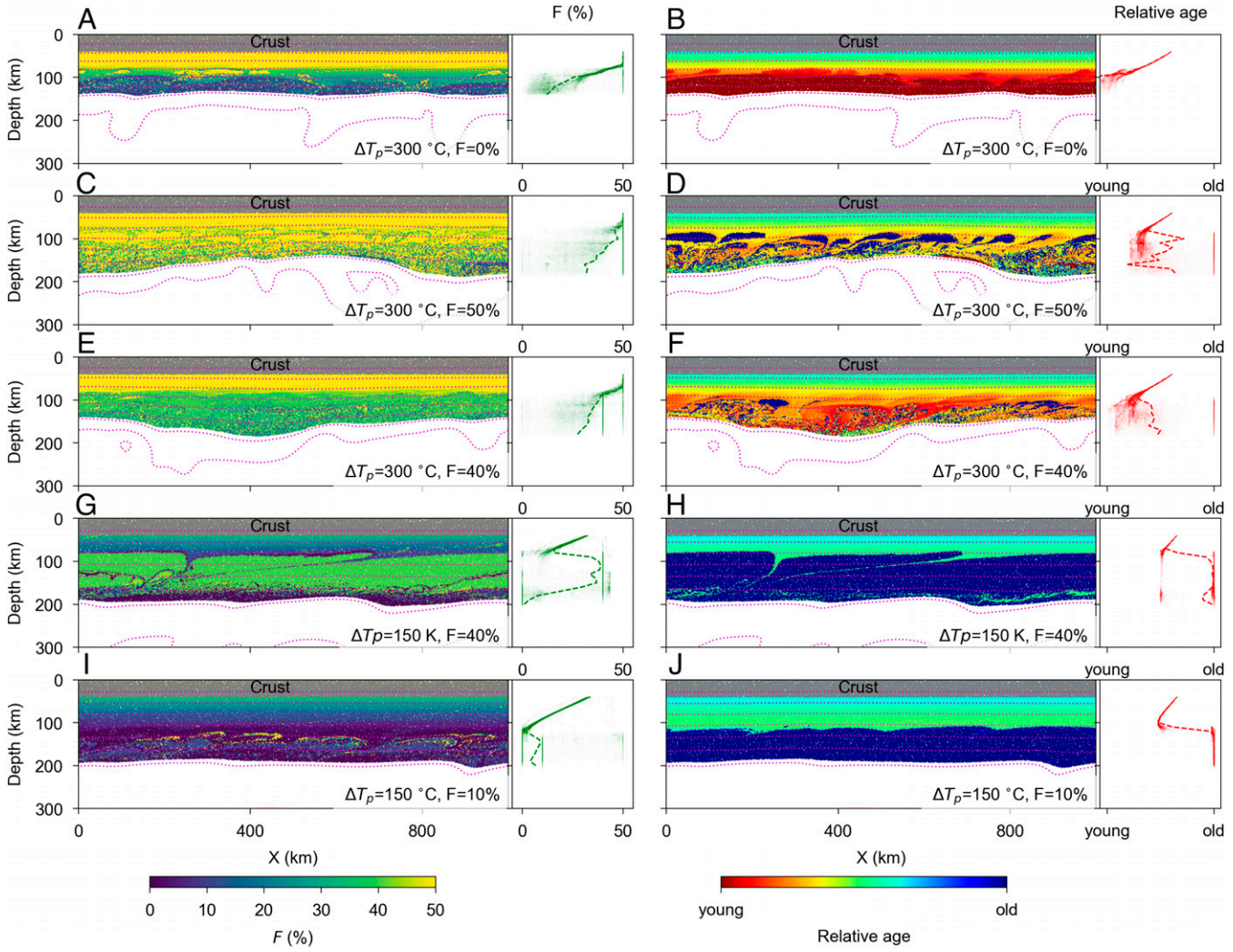

Fig. 4. Modeled composition and age structure of CLM ~1,200 Myr after delamination. (*A* and *B*) No relamination, depletion degree (*A*) and age (*B*) change linearly with depth; the lithosphere is very thin. (*C* and *D*) Relamination with large CLM depletion degree and high mantle temperature; highly depleted (*C*), ancient (*D*) CLM materials are relaminated to the growing lithosphere to form a thick depleted lithospheric root. (*E* and *F*) Relamination with small CLM depletion degree and high mantle temperature; two-layer models are formed in its composition (*E*) and age structures (*F*), with ancient fertile materials incorporated beneath a young depleted growing lid. (*G* and *H*) Relamination with relatively large CLM depletion degree and low mantle temperature; two-layer models are formed in its composition (*G*) and age structures (*H*), with ancient depleted materials incorporated beneath a young fertile growing lid. (*I* and *J*) Relamination with low CLM depletion degree and low mantle temperature; two-layer models are also formed in its composition (*I*) and age structures (*J*), with ancient fertile materials incorporated beneath a young fertile growing lid. Green points and dashed lines on the right side of *A*, *C*, *E*, *G*, *I* denote the depletion degree of CLM tracers and their average value at different depths, respectively. Red points and dashed lines on the right side of *B*, *D*, *F*, *H*, *J* denote the relative age of CLM tracers and their average value at different depths, respectively.

ages of upwelled CLM relicts and likely explain the chronologically apparent disappearance of the Hadean lithospheric mantle (9, 61).

Massive Regional Relamination: Constraints from Composition. The xenoliths record of the lithospheric mantle of both Archean and Proterozoic cratons shows that the distribution of the depletion degree is heterogeneous and may vary with depth. Some locations (e.g., Lesotho, Limpopo, Botswana, and Siberia) (Fig. 5*C*) preserve highly depleted peridotites at middle-lower depth but fertile peridotites at shallower depth, whereas in other cratonic keels (e.g., Slave and Kaapvaal) (Fig. 5*D*), the layering of depleted and fertile peridotites is inverted (6, 8). Subduction and convergence can effectively explain the transportation of large amounts of shallow, highly depleted residue to the deep (5, 9). However, the imbricated/dipping lithospheric structure formed by subduction stacking (63) is not easily reconciled with the horizontally layered depletion structure of the existing lithospheric mantle (64), while the abundance of oceanic crust eclogites according to the subduction model (1) is also significantly different from their detectable, relatively small abundance via geophysical studies and xenolith records (64). A recently proposed subduction-related viscous underplating model (6) with viscous drainage of eclogites (65) can potentially solve these contradictions. However, this explanation critically relies on the operation of subduction and convergence in the early Earth. The duration of early stagnant lid and onset time of large-scale subduction (Hadean to Neoproterozoic) are controversial (35–38), and it remains debated whether subduction could have been relevant to the formation of cratons during the Mesoarchean to Neoarchean or earlier (9, 61). Accordingly, the interpretation of the compositional structure of cratonic lithosphere via subduction remains problematic.

Other mechanisms could also lead to heterogeneous CLM, such as rifting and mantle plumes (7, 66). Rifting events may progressively thin the lithosphere, allow for decompression melting, and add bodies of variable shape, age, and depletion degree to the lithosphere (7). A similar result may be due to the effect

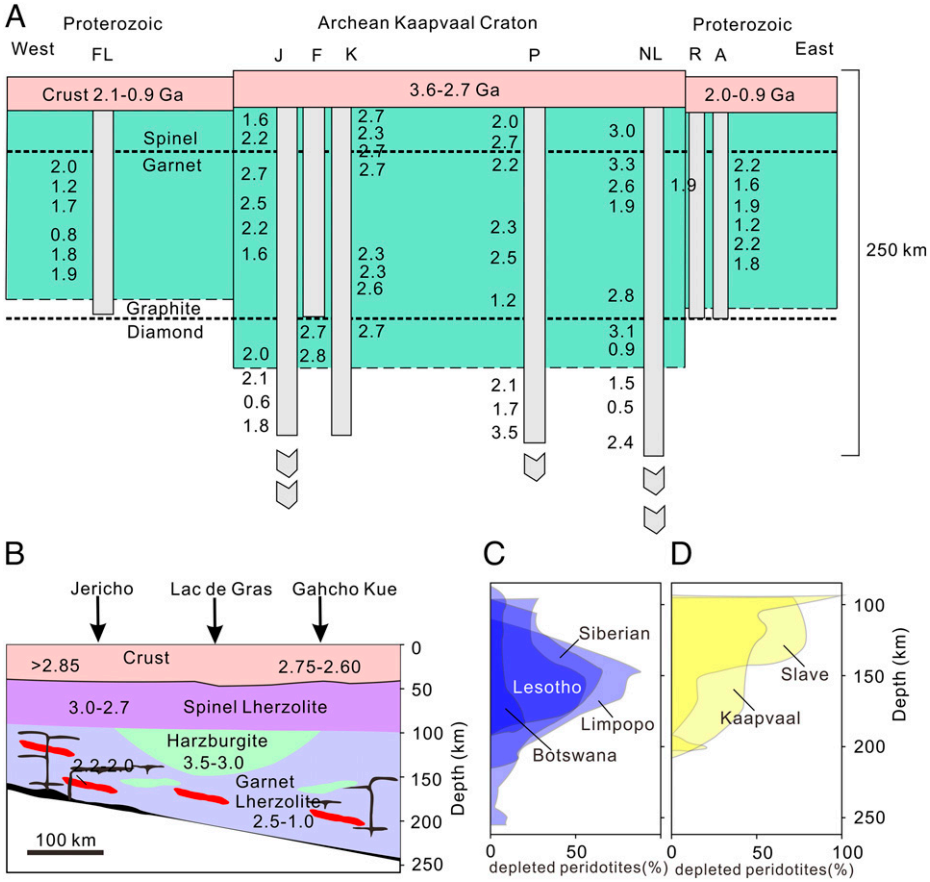

Fig. 5. Age and depletion architecture of lithospheric mantle in Kaapvaal, Slave, and other cratons. (*A*) Distribution of rock ages in the lithospheric mantle of South Africa determined by geochronological measurements, showing complex age structure without a strict time order (5). FL, Farm Louwrencia; J, Jagersfontein; F, Finsch; K, Kimberley; P, Premier; NL, North Lesotho; R, Ramatšeliso; A, Abbotsford. (*B*) Age and composition structure below the Slave Craton (55). The numbers in *A* and *B* are ages in Ga. (*C*) Depleted layers in the middle to lower part of the lithospheric mantle in some cratonic areas (6). (*D*) Depleted layers in the upper part of the lithospheric mantle in some cratonic areas (6).

of a plume providing excess temperature beneath a thinned lithosphere (66), although this model cannot explain heterogeneous age distribution. Both models explain major high-degree shallow melting beneath a thinned lithosphere. Here, we suggest that in the growth of the thermal boundary layer, during cooling, additional heterogeneities can be embedded in the lithosphere due to MRR.

More generally, the MRR model (Fig. 4 *A*, *C*, *E*, *G*, and *I*) explains different compositional layering structures, compatible with those observed (Fig. 5 *B*–*D*), that may occur in conjunction with other mechanisms and is independent of the tectonic regime. First, the foundering of the CLM is viable under all tectonic regimes proposed for the early Earth (21, 37, 64, 67). Mantle mixing and upwelling of CLM are embedded in general mantle circulation models and do not require or refute the operation of plate tectonics or any other proposed preplate tectonic regimes. Although these may differ in lithospheric formation processes (6, 7, 34, 45), the conditions for mantle convection and mixing are independent and instead depend on the factors modeled here, that is, mantle temperature and temperature- and composition-dependent buoyancy (68). Thus, MRR remains a viable mechanism, independent of the operation of subduction, that best explains the formation of large heterogeneities of the continental lithospheric mantle throughout Earth's history. In particular, MRR can explain the occurrence of a depleted upper layer atop a fertile layer (Fig. 4 *A*, *C*, and *E*) as observed in the Slave Craton (Fig. 5*C*) or the emplacement of a depleted lower layer beneath a fertile one (Fig. 4*G*), as observed in the Siberian Craton (Fig. 5*D*). Additionally, while MRR events incorporate the deeply foundered CLM relicts into the newly constructed lithosphere, they can also entrain some deep materials, suggesting an explanation for the puzzling coexistence of ultra-deep source materials and shallow, low-pressure melting residues under some cratons, such as the Slave Craton (19, 59).

MRR incorporates the foundered CLM under the growing lithosphere, preserving paleo lithosphere-asthenosphere boundary materials at the middle depth of the composite lithosphere, which can form a structure similar to the seismically detected mid-lithosphere discontinuity (MLD) (40, 69, 70). For example, an MLD is detected below the Ontong Java oceanic plateau at depths between the newly formed oceanic lithosphere and underplating material containing ancient CLM relicts (14, 40, 71). Seismic studies show that multiple MLD structures may exist under the Kaapvaal, North American, and Australian cratons (72–74). The nature of the MLD is not uniform (69, 70), and the MRR mechanism proposed here can readily explain the formation of some multiple subhorizontal MLDs in between relaminated layers and blocks. Thus, MRR remains a viable mechanism, independent of the operation of subduction, that best explains the formation of large heterogeneities of the continental lithospheric mantle throughout Earth's history.

The Role of Massive Regional Relamination in CLM Accretion. Episodic MRR events (Figs. 4 and 6*E*) may be a relevant mechanism to explain the observed complex lithospheric heterogeneities

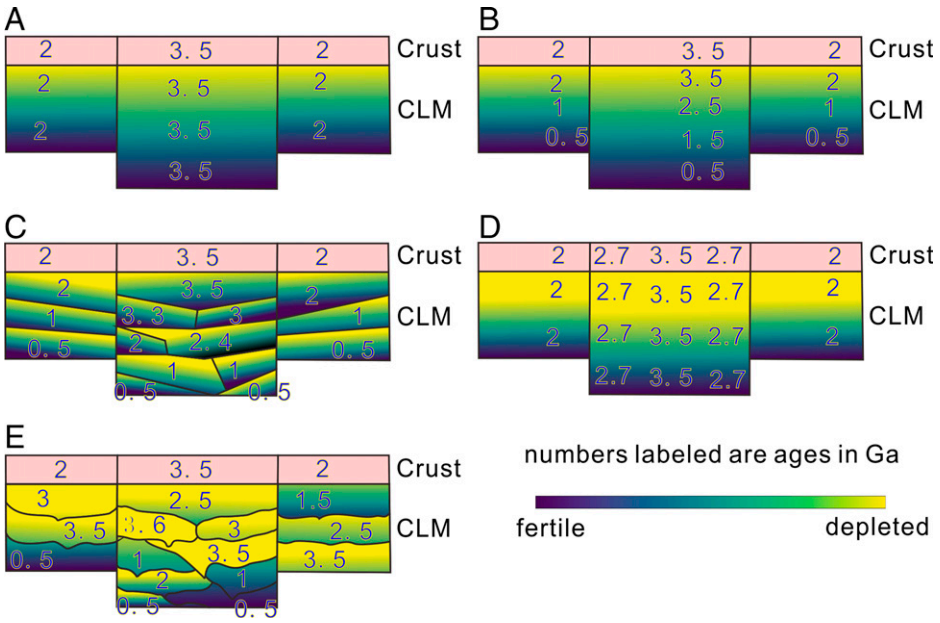

Fig. 6. Age and depletion architecture of lithospheric mantle constructed by different mechanisms [modified after Pearson, 1999 (5)]. (*A*) Rapid plume or rapid subduction. (*B*) Underplating: cooling or magmatic. (*C*) Subduction accretion. (*D*) Lateral "block" accretion. (*E*) Repeated MRR events proposed in this study. *A*–*D* are with strict time order. *A* or *D* has consistent age from top to bottom of each cratonic block, and *B* or *C* has decreasing ages from top to bottom of each cratonic block. In contrast, only *E* is without strict time order. *A, B,* and *D* have depletion structures inherited from the craton formation, possibly increasing with shallowing depth (horizontally stratified) (64). *C* has imbricated dipping depletion structures inherited from slab imbrication. *E* has horizontally stratified depletion structures perturbed by MRR; the types of depletion changing with depth can vary (see Fig. 4).

described above (Fig. 5). This mechanism overcomes the limitations of other lithosphere formation mechanisms (3, 5) that imply a strict time order and specific compositional structures (Fig. 6 *A*–*D*). The upwelled CLM relicts below cratons, orogenic belts, and oceanic basins, emplaced via MRR events, can be foundered into the deep mantle repeatedly if attaining enough negative buoyancy during renewed delamination or ocean closure, which can result in new foundering-MRR cycles until the CLM relicts are disrupted in the ambient mantle or finally anchored below stable cratons. These foundering-MRR cycles keep the CLM volumetric balance between the continental lithospheric mantle and the deep mantle, contributing to the longevity of continents. This means that the relaminating CLM in later cold MRR events (e.g., Fig. 4 *G*–*J*) is actually the foundered CLM reconstructed in earlier hot MRR events (e.g., Fig. 4 *A*–*F*); thus, the newly formed CLM should have finer structures (formed in earlier MRR events) than those shown in Fig. 4 *G*–*J*.

The existing CLM relicts below different tectonic units show that some cratons were not as stable as previously understood (2, 10, 58), especially the lithospheric mantle (9, 40, 58, 75–77). The relative stability of the cold crustal section of cratons is likely accompanied by the foundering-MRR cycles at mantle depths, especially during the cratonization stage, when complex CLM structures were formed. This also means that the evolution of CLM is probably a competitive process between constructive MRR and destructive foundering. This process makes any Hadean lithospheric mantle materials reset their ages during the hot MRR events, whereas the majority of Archean cratons and the minority of Proterozoic cratons exchange their CLM during the warm to cold MRR events, respectively

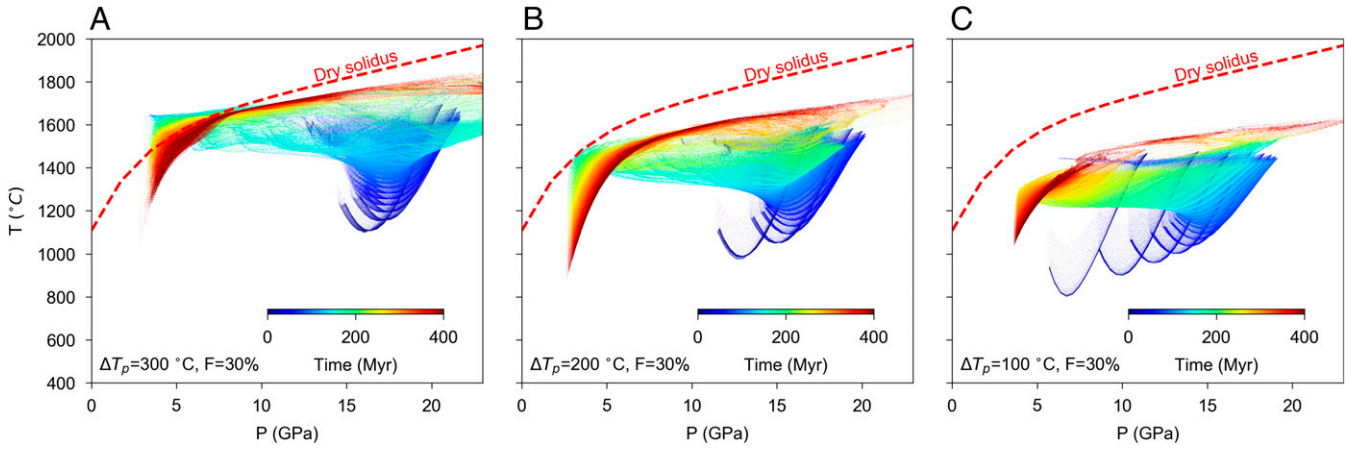

Fig. 7. Pressure-Temperature-time (P-T-t) paths of CLM tracers during their MRR under different mantle T_ps. (*A*) Hot MRR; many tracers can surpass the dry solidus (red dashed lines) of peridotites (62) during their MRR and reset their ages. (*B*) Hot/warm MRR; few tracers can surpass the dry solidus and reset their ages. (*C*) Warm-cold MRR; no tracers can surpass the dry solidus and reset their ages.

(Fig. 7). Some ongoing Phanerozoic proposed cratonization processes in the Altaids, Tibet, and other places are likely accompanied by such delamination (9, 78–80) and relamination processes (49, 50) as well. In this process, the plateaus or orogenic belts lose their primitive dense CLM and replace it with hybrid buoyant materials containing ancient CLM relicts detached from cratonic units. The models also show that CLM segments delaminated in the Phanerozoic may still be in their sinking or stagnation stage (Fig. 3*B*); thus, their temperature-related fast anomalies (Fig. 1 *C*, *I*, and *O*) can still be detected. Some fast anomalies in the mantle, especially those unrelated to subducting slabs, such as those in the mantle transition zone beneath North China, West African cratons, and their adjacent regions (27, 28), can be explained by delaminated or stagnating CLM relicts. In this context, the process proposed here may contribute significantly to the coupled evolution of a heterogeneous lithosphere and mantle.

The foundering-MRR cycle is likely an important mechanism for density-driven differentiation, which can convert such high-density orogens to buoyant cratons (81). In these cycles, high-density eclogites can be left in the deep, whereas buoyant depleted peridotites can be incorporated into the lithosphere via MRR. This can explain the eclogite abundance and compositional stratification problems in the subduction imbrication model discussed above (64). The foundering-MRR cycle of most depleted CLM segments mainly takes place in the shallow mantle (Fig. 3*A*), whereas fertile peridotite can be recycled into lower mantle depths. These processes are conducive to mantle stratification and are important to the formation of the shallow depleted mantle. With the secular cooling of the Earth's mantle, the feasibility and frequency of delamination and thus MRR are decreasing (34). This means that previously formed cratons are becoming more stable than before, and the architectures of future cratons will not be as complex as those formed in the Archean.

The types and triggers of removal and sinking of the depleted CLM are various, ranging from convective removal to sagduction, delamination, dripping, and subduction (15, 82–84). Thus, the foundered block may have different sizes and contain the eclogitized lower crust or contain only the lower mantle lithosphere below the MLD (18, 39, 75, 85), which may lead to different MRR modalities (6, 7, 15). The deformation, transportation, disruption, and sinking/stagnation depth of the foundered CLM is similar to those of the subducting slab, which are affected by many factors, including viscosity and density changes or jumps induced by water, Mg content, phase transition, Clapeyron slope, partial melting, CLM eclogite content, depletion degree, metastable-olivine, and specific slab dynamics (segmentation, folding, or piling) (43, 86–88). These complex factors add not only variabilities to the MRR model but also complexities to the heterogeneity of the lithosphere and deep mantle, which have been covered by our simplified setup. This also extends the applicability of MRR and needs considerable future work. As long as the depleted lithosphere is not completely mixed or refertilized, the potential of MRR caused by depletion-related buoyancy always exists, and the relamination of such CLM fragments is just a matter of time. Although MRR is not the only way to create heterogeneous CLM, it is compatible with other mechanisms.

Materials and Methods

The evolution of thermal and chemical anomalies of the CLM in the viscous mantle is modeled here as the Stokes flow of an incompressible fluid, solving for the conservation of mass, momentum, and energy using the geodynamic computational frame Underworld (89). This method embeds Lagrangian particles in a Cartesian Finite Element mesh, tracing thermo-chemical conditions relevant for the problem treated here (*SI Appendix*, sections 1 and 2).

We designed two modeling groups: a sensitivity test group and a main group. The sensitivity test group (*SI Appendix*, section 3) aimed to test the sensitivity of the model to the parameters described above, including block length and thickness, ΔT_p, V_{surf}, F, η_{max}, and f_{vis}, whereas the main group (*SI Appendix*, section 4) aimed to investigate the evolution of a thick (160-km) cratonic block sinking in the dry ambient mantle with no water- or fluid-related weakening, following previous works (18, 44).

Data, Materials, and Software Availability. All numerical modeling data were calculated using Underworld2 (https://doi.org/10.5281/zenodo.3384283) (90). All study data are included in the article and/or *SI Appendix*.

ACKNOWLEDGMENTS. This study was supported by the National Natural Science Foundation of China (Grant Nos. 42272243, 41890834, and 41802217) and Most Special Fund from the State Key Laboratory of Geological Processes and Mineral Resources (Grant No. MSFGPMR02-3). The calculation/modeling work in this article used the Goody-1 high performance cluster of the School of Earth Science at the China University of Geosciences.

Author affiliations: [a]State Key Lab of Geological Processes and Mineral Resources, Center for Global Tectonics, School of Earth Sciences, China University of Geosciences, Wuhan, 430074 China; [b]School of Earth, Atmosphere and Environment, Monash University, Clayton, 3800 VIC, Australia; and [c]Badong National Observatory and Research Station for Geohazards, China University of Geosciences, Wuhan, 430074 China

1. C. Herzberg, R. Rudnick, Formation of cratonic lithosphere: An integrated thermal and petrological model. *Lithos* **149**, 4–15 (2012).
2. C. A. Lee, P. Luffi, E. J. Chin, Building and destroying continental mantle. *Annu. Rev. Earth Planet. Sci.* **39**, 59–90 (2011).
3. D. G. Pearson, N. Wittig, "The formation and evolution of cratonic mantle lithosphere:evidence from mantle xenoliths" in *Treatise on Geochemistry*, H. D. Holl, K. K. Turekian, Eds. (Elsevier, ed. 2, 2014), Chap. 3, pp. 255–292.
4. T. M. Kusky *et al.*, Insights into the tectonic evolution of the north China craton through comparative tectonic analysis: A record of outward growth of Precambrian continents. *Earth Sci. Rev.* **162**, 387–432 (2016).
5. D. G. Pearson, The age of continental roots. *Lithos* **24**, 171–194 (1999).
6. A. L. Perchuk, T. V. Gerya, V. S. Zakharov, W. L. Griffin, Building cratonic keels in Precambrian plate tectonics. *Nature* **586**, 395–401 (2020).
7. F. A. Capitanio, O. Nebel, P. A. Cawood, Thermochemical lithosphere differentiation and the origin of cratonic mantle. *Nature* **588**, 89–94 (2020).
8. S. Y. O'Reilly, W. L. Griffin, Imaging global chemical and thermal heterogeneity in the subcontinental lithospheric mantle with garnets and xenoliths: Geophysical implications. *Tectonophysics* **416**, 289–309 (2006).
9. D. G. Pearson *et al.*, Deep continental roots and cratons. *Nature* **596**, 199–210 (2021).
10. R. Zhu, G. Zhao, W. Xiao, L. Chen, Y. Tang, Origin, accretion, and reworking of continents. *Rev. Geophys.* **59**, e2019R–e2689R (2021).
11. A. Luguet *et al.*, An integrated petrological, geochemical and Re–Os isotope study of peridotite xenoliths from the Argyle lamproite, Western Australia and implications for cratonic diamond occurrences. *Lithos* **112**, 1096–1108 (2009).
12. N. Wittig *et al.*, Formation of the North Atlantic craton: Timing and mechanisms constrained from Re–Os isotope and PGE data of peridotite xenoliths from SW Greenland. *Chem. Geol.* **276**, 166–187 (2010).
13. M. Coltorti, C. Bonadiman, S. Y. O'Reilly, W. L. Griffin, N. J. Pearson, Buoyant ancient continental mantle embedded in oceanic lithosphere (Sal Island, Cape Verde Archipelago). *Lithos* **120**, 223–233 (2010).
14. A. Ishikawa, D. G. Pearson, C. W. Dale, Ancient Os isotope signatures from the Ontong Java Plateau lithosphere: Tracing lithospheric accretion history. *Earth Planet. Sci. Lett.* **301**, 159–170 (2011).
15. C. Z. Liu *et al.*, Archean cratonic mantle recycled at a mid-ocean ridge. *Sci. Adv.* **8**, eabn6749 (2022).
16. H. Zhou, H. J. B. Dick, Thin crust as evidence for depleted mantle supporting the Marion Rise. *Nature* **494**, 195–200 (2013).
17. J. Liu, J. M. Scott, C. E. Martin, D. G. Pearson, The longevity of Archean mantle residues in the convecting upper mantle and their role in young continent formation. *Earth Planet. Sci. Lett.* **424**, 109–118 (2015).
18. L. Peng, L. Liu, L. Liu, The fate of delaminated cratonic lithosphere. *Earth Planet. Sci. Lett.* **594**, 117740 (2022).
19. W. L. Griffin *et al.*, Layered mantle lithosphere in the Lac de Gras Area, Slave craton: Composition, structure and origin. *J. Petrol.* **40**, 705–727 (1999).

20. A. Stracke, F. Genske, J. Berndt, J. M. Koornneef, Ubiquitous ultra-depleted domains in Earth's mantle. *Nat. Geosci.* **12**, 851–855 (2019).
21. R. L. Rudnick, Making continental crust. *Nature* **378**, 571–578 (1995).
22. S. Gao *et al.*, Recycling lower continental crust in the North China craton. *Nature* **432**, 892–897 (2004).
23. T. Nakagawa, P. J. Tackley, F. Deschamps, J. A. D. Connolly, The influence of MORB and harzburgite composition on thermo-chemical mantle convection in a 3-D spherical shell with self-consistently calculated mineral physics. *Earth Planet. Sci. Lett.* **296**, 403–412 (2010).
24. P. J. Tackley, Strong heterogeneity caused by deep mantle layering. *Geochem. Geophys. Geosyst.* **3**, 1–22 (2002).
25. C. A. Lee, Compositional variation of density and seismic velocities in natural peridotites at STP conditions: Implications for seismic imaging of compositional heterogeneities in the upper mantle. *J. Geophys. Res. Solid Earth*, 10.1029/2003JB002413 (2003).
26. D. L. Anderson, Speculations on the nature and cause of mantle heterogeneity. *Tectonophysics* **416**, 7–22 (2006).
27. M. J. Bezada *et al.*, Piecewise delamination of Moroccan lithosphere from beneath the Atlas Mountains. *Geochem. Geophys. Geosyst.* **15**, 975–985 (2014).
28. J. Lei, Upper-mantle tomography and dynamics beneath the North China craton. *J. Geophys. Res. Solid Earth* **117**, 10–1029 (2012).
29. P. Olson, D. A. Yuen, D. Balsiger, Mixing of passive heterogeneities by mantle convection. *J. Geophys. Res. Solid Earth* **89**, 425–436 (1984).
30. P. E. van Keken, E. H. Hauri, C. J. Ballentine, Mantle mixing: The generation, preservation, and destruction of chemical heterogeneity. *Annu. Rev. Earth Planet. Sci.* **30**, 493–525 (2002).
31. C. Herzberg, K. Condie, J. Korenaga, Thermal history of the Earth and its petrological expression. *Earth Planet. Sci. Lett.* **292**, 79–88 (2010).
32. C. Z. Liu *et al.*, Ancient, highly heterogeneous mantle beneath Gakkel ridge, Arctic Ocean. *Nature* **452**, 311–316 (2008).
33. S. Aulbach, N. T. Arndt, Eclogites as palaeodynamic archives: Evidence for warm (not hot) and depleted (but heterogeneous) Archaean ambient mantle. *Earth Planet. Sci. Lett.* **505**, 162–172 (2019).
34. P. Chowdhury, T. Gerya, S. Chakraborty, Emergence of silicic continents as the lower crust peels off on a hot plate-tectonic Earth. *Nat. Geosci.* **10**, 698–703 (2017).
35. M. Brown, T. Johnson, N. J. Gardiner, Plate tectonics and the Archean Earth. *Annu. Rev. Earth Planet. Sci.* **48**, 291–320 (2020).
36. B. F. Windley, T. Kusky, A. Polat, Onset of plate tectonics by the Eoarchean. *Precambrian Res.* **352**, 105980 (2021).
37. P. A. Cawood *et al.*, Geological archive of the onset of plate tectonics. *Philos. Trans. A Math. Phys. Eng. Sci.* **376**, 20170405 (2018).
38. R. J. Stern, The evolution of plate tectonics. *Philos. Trans. A Math. Phys. Eng. Sci.* **376**, 20170406 (2018).
39. Y. Shi, Z. Li, L. Chen, J. P. Morgan, Connection between a subcontinental plume and the mid-lithospheric discontinuity leads to fast and intense craton lithospheric thinning. *Tectonics* **40**, e2021T–e6711T (2021).
40. Z. Wang, T. M. Kusky, The importance of a weak mid-lithospheric layer on the evolution of the cratonic lithosphere. *Earth Sci. Rev.* **190**, 557–569 (2019).
41. A. L. Perchuk, T. V. Gerya, V. S. Zakharov, W. L. Griffin, Depletion of the upper mantle by convergent tectonics in the Early Earth. *Sci. Rep.* **11**, 21489 (2021).
42. C. T. Lee, Q. Yin, R. L. Rudnick, S. B. Jacobsen, Preservation of ancient and fertile lithospheric mantle beneath the southwestern United States. *Nature* **411**, 69–73 (2001).
43. M. D. Ballmer, N. C. Schmerr, T. Nakagawa, J. Ritsema, Compositional mantle layering revealed by slab stagnation at ~1000-km depth. *Sci. Adv.* **1**, e1500815 (2015).
44. G. Hirth, D. Kohlstedt, "Rheology of the upper mantle and the mantle wedge: A view from the experimentalists" in Inside the Subduction Factory, J. Eiler (American Geophysical Union, 2004) vol. 138, pp. 83–105.
45. H. Wang, J. van Hunen, D. G. Pearson, Making Archean cratonic roots by lateral compression: A two-stage thickening and stabilization model. *Tectonophysics* **746**, 562–571 (2018).
46. P. Maierová, K. Schulmann, T. Gerya, Relamination styles in collisional orogens. *Tectonics* **37**, 224–250 (2018).
47. B. R. Hacker, P. B. Kelemen, M. D. Behn, Differentiation of the continental crust by relamination. *Earth Planet. Sci. Lett.* **307**, 501–516 (2011).
48. P. Olson, D. A. Yuen, D. Balsiger, Convective mixing and the fine structure of mantle heterogeneity. *Phys. Earth Planet. Inter.* **36**, 291–304 (1984).
49. G. Feng, J. Yang, Y. Dilek, F. Liu, F. Xiong, Petrological and Re-Os isotopic constraints on the origin and tectonic setting of the Cuobuzha peridotite, Yarlung Zangbo suture zone, southwest Tibet, China. *Lithosphere* **10**, 95–108 (2017).
50. Y. Xu *et al.*, The complex life cycle of oceanic lithosphere: A study of Yarlung-Zangbo ophiolitic peridotites, Tibet. *Geochim. Cosmochim. Acta* **277**, 175–191 (2020).
51. M. Bizimis, M. Griselin, J. C. Lassiter, V. J. M. Salters, G. Sen, Ancient recycled mantle lithosphere in the Hawaiian plume: Osmium–Hafnium isotopic evidence from peridotite mantle xenoliths. *Earth Planet. Sci. Lett.* **257**, 259–273 (2007).
52. E. Bonatti, Subcontinental mantle exposed in the Atlantic Ocean on St Peter-Paul islets. *Nature* **345**, 800–802 (1990).
53. J. Harvey *et al.*, Ancient melt extraction from the oceanic upper mantle revealed by Re–Os isotopes in abyssal peridotites from the Mid-Atlantic ridge. *Earth Planet. Sci. Lett.* **244**, 606–621 (2006).
54. K. Hanghøj, P. Kelemen, S. Bernstein, J. Blusztajn, R. Frei, Osmium isotopes in the Wiedemann Fjord mantle xenoliths: A unique record of cratonic mantle formation by melt depletion in the Archaean. *Geochem. Geophys. Geosyst.*, 10.1029/2000GC000085 (2001).
55. L. M. Heaman, D. G. Pearson, Nature and evolution of the Slave Province subcontinental lithospheric mantle. *Can. J. Earth Sci.* **47**, 369–388 (2010).
56. K. J. Westerlund *et al.*, A subduction wedge origin for Paleoarchean peridotitic diamonds and harzburgites from the Panda kimberlite, Slave craton: Evidence from Re–Os isotope systematics. *Contrib. Mineral. Petrol.* **152**, 275 (2006).
57. J. Czas, D. G. Pearson, T. Stachel, B. A. Kjarsgaard, G. H. Read, A Palaeoproterozoic diamond-bearing lithospheric mantle root beneath the Archean Sask craton, Canada. *Lithos* **356-357**, 105301 (2020).
58. S. Gao, R. L. Rudnick, R. W. Carlson, W. F. McDonough, Y. Liu, Re–Os evidence for replacement of ancient mantle lithosphere beneath the North China craton. *Earth Planet. Sci. Lett.* **198**, 307–322 (2002).
59. D. G. Pearson, N. Wittig, Formation of Archaean continental lithosphere and its diamonds: The root of the problem. *J. Geol. Soc. London* **165**, 895–914 (2008).
60. D. G. Pearson, S. W. Parman, G. M. Nowell, A link between large mantle melting events and continent growth seen in osmium isotopes. *Nature* **449**, 202–205 (2007).
61. W. L. Griffin, S. Y. O'Reilly, "The earliest subcontinental lithospheric mantle" in *Earth's Oldest Rocks*, M. J. Van Kranendonk, V. C. Bennett, J. E. Hoffmann, Eds. (Elsevier, ed. 2, 2019), Chap. 5, pp. 81–102.
62. D. Andrault *et al.*, Deep and persistent melt layer in the Archaean mantle. *Nat. Geosci.* **11**, 139–143 (2018).
63. H. Helmstaedt, D. J. Schulze, Data from "Southern African kimberlites and their mantle sample: Implications for Archean tectonics and lithosphere evolution." Geological Society of Australia, Special Publication 14, 358–368 (1989).
64. C. T. A. Lee, Geochemical/petrologic constraints on the origin of cratonic mantle. *Archean Geodyn. Environ.* **164**, 89–114 (2006).
65. Z. Wang, T. Kusky, L. Wang, Long-lasting viscous drainage of eclogites from the cratonic lithospheric mantle after Archean subduction stacking. *Geology* **50**, 583–587 (2022).
66. J. Liu *et al.*, Plume-driven recratonization of deep continental lithospheric mantle. *Nature* **592**, 732–736 (2021).
67. P. Chowdhury, S. Chakraborty, T. V. Gerya, P. A. Cawood, F. A. Capitanio, Peel-back controlled lithospheric convergence explains the secular transitions in Archean metamorphism and magmatism. *Earth Planet. Sci. Lett.* **538**, 116224 (2020).
68. A. Lenardic, The diversity of tectonic modes and thoughts about transitions between them. *Philos. Trans. A Math. Phys. Eng. Sci.* **376**, 20170416 (2018).
69. S. Aulbach, M. Massuyeau, F. Gaillard, Origins of cratonic mantle discontinuities: A view from petrology, geochemistry and thermodynamic models. *Lithos* **268**, 364–382 (2017).
70. K. Selway, H. Ford, P. Kelemen, The seismic mid-lithosphere discontinuity. *Earth Planet. Sci. Lett.* **414**, 45–57 (2015).
71. S. Tharimena, C. A. Rychert, N. Harmon, Seismic imaging of a mid-lithospheric discontinuity beneath Ontong Java Plateau. *Earth Planet. Sci. Lett.* **450**, 62–70 (2016).
72. A. Birkey, H. A. Ford, P. Dabney, G. Goldhagen, The lithospheric architecture of Australia from seismic receiver functions. *J. Geophys. Res. Solid Earth* **126**, e2020JB020999 (2021).
73. M. Calò, T. Bodin, B. Romanowicz, Layered structure in the upper mantle across North America from joint inversion of long and short period seismic data. *Earth Planet. Sci. Lett.* **449**, 164–175 (2016).
74. F. Sodoudi *et al.*, Seismic evidence for stratification in composition and anisotropic fabric within the thick lithosphere of Kalahari craton. *Geochem. Geophys. Geosyst.* **14**, 5393–5412 (2013).
75. Z. Wang, T. Kusky, F. Capitanio, On the role of lower crust and mid-lithosphere discontinuity for cratonic lithosphere delamination and recycling. *Geophys. Res. Lett.* **15**, 7425–7433 (2018).
76. M. K. Kaban, W. D. Mooney, A. G. Petrunin, Cratonic root beneath North America shifted by basal drag from the convecting mantle. *Nat. Geosci.* **8**, 797–800 (2015).
77. Z. Wang, T. Kusky, F. Capitanio, Ancient continental lithosphere dislocated beneath ocean basins along the mid-lithosphere discontinuity: A hypothesis. *Geophys. Res. Lett.* **44**, 9253–9260 (2017).
78. R. Kind *et al.*, Scandinavia: A former Tibet? *Geochem. Geophys. Geosyst.* **14**, 4479–4487 (2013).
79. A. M. C. Şengör, N. Lom, A. Polat, The nature and origin of cratons constrained by their surface geology. *Geol. Soc. Am. Bull.* **134**, 1485–1505 (2021).
80. A. Yin, T. M. Harrison, Geologic evolution of the Himalayan-Tibetan orogen. *Annu. Rev. Earth Planet. Sci.* **28**, 211–280 (2000).
81. T. M. Kusky, B. F. Windley, M. Zhai, Tectonic evolution of the North China Block: From orogen to craton to orogen. *Geol. Soc. Lond. Spec. Publ.* **280**, 1–34 (2007).
82. O. H. Göğüş, R. N. Pysklywec, Mantle lithosphere delamination driving plateau uplift and synconvergent extension in eastern Anatolia. *Geology* **36**, 723–726 (2008).
83. T. Gerya, Geodynamics of the early Earth: Quest for the missing paradigm. *Geology* **47**, 1006–1007 (2019).
84. A. Roman, N. Arndt, Differentiated Archean oceanic crust: Its thermal structure, mechanical stability and a test of the sagduction hypothesis. *Geochim. Cosmochim. Acta* **278**, 65–77 (2020).
85. L. Liu, J. P. Morgan, Y. Xu, M. Menzies, Craton destruction part I: Cratonic keel delamination along a weak mid-lithospheric discontinuity layer. *J. Geophys. Res. Solid Earth* **123**, 10040–10068 (2018).
86. S. Goes, R. Agrusta, J. van Hunen, F. Garel, Subduction-transition zone interaction: A review. *Geosphere* **13**, 644–664 (2017).
87. Z. Li, T. Gerya, J. A. D. Connolly, Variability of subducting slab morphologies in the mantle transition zone: Insight from petrological-thermomechanical modeling. *Earth Sci. Rev.* **196**, 102874 (2019).
88. T. V. Gerya, D. Bercovici, T. W. Becker, Dynamic slab segmentation due to brittle-ductile damage in the outer rise. *Nature* **599**, 245–250 (2021).
89. L. Moresi, F. Dufour, H. Mühlhaus, A Lagrangian integration point finite element method for large deformation modeling of viscoelastic geomaterials. *J. Comput. Phys.* **184**, 476–497 (2003).
90. J. Mansour, underworldcode/underworld2: v2.8.1b. Zenodo. https://zenodo.org/record/3384283. Deposited 2 September 2019.